AIP | Applied Physics Letters

Infrared lasing in InN nanobelts

Ming-Shien Hu, Geng-Ming Hsu, Kuei-Hsien Chen, Chia-Ju Yu, Hsu-Cheng Hsu, Li-Chyong Chen, Jih-Shang Hwang, Lu-Sheng Hong, and Yang-Fang Chen

Citation: Applied Physics Letters **90**, 123109 (2007); doi: 10.1063/1.2714291
View online: http://dx.doi.org/10.1063/1.2714291
View Table of Contents: http://scitation.aip.org/content/aip/journal/apl/90/12?ver=pdfcov
Published by the AIP Publishing

Infrared lasing in InN nanobelts

Ming-Shien Hu, Geng-Ming Hsu, and Kuei-Hsien Chen[a),b)]
Institute of Atomic and Molecular Sciences, Academia Sinica, Taipei 10617, Taiwan

Chia-Ju Yu, Hsu-Cheng Hsu, and Li-Chyong Chen[a),c)]
Center for Condensed Matter Sciences, National Taiwan University, Taipei 10617, Taiwan

Jih-Shang Hwang
Institute of Optoelectronic Sciences, National Taiwan Ocean University, Keelung 20224, Taiwan

Lu-Sheng Hong
Department of Chemical Engineering, National Taiwan University of Science and Technology, Taipei 10607, Taiwan

Yang-Fang Chen
Department of Physics, National Taiwan University, Taipei 10617, Taiwan

(Received 28 October 2006; accepted 10 February 2007; published online 21 March 2007)

Infrared lasing from single-crystalline InN nanobelts grown by metal organic chemical vapor deposition was demonstrated. Transmission electron microscopy studies revealed that the InN nanobelts of rectangular cross section grew along [110] direction and were enclosed by $\pm(001)$ and $\pm(1\bar{1}0)$ planes. The infrared lasing action was observed at 20 K in the InN nanobelts grown on an amorphous silicon nitride coated silicon substrate by continuous wave laser pumping. © *2007 American Institute of Physics*. [DOI: 10.1063/1.2714291]

Indium nitride (InN) is a promising semiconductor which can be used in many potential applications, such as high frequency electronic devices,[1] light emitting diodes,[2,3] and solar cells.[4] Recently, InN has received more attention due to the growing debate over the revision of its fundamental band gap from visible (1.8–2.1 eV) to infrared (0.7–0.8 eV) spectral range,[5] although some minor controversy remained.[6] Actually, resolving the band gap controversy as well as realizing the device fabrication strongly rely on the growth of high quality crystal of InN. Nevertheless, it is still a challenging task due to the extremely high equilibrium vapor pressure of nitrogen and the low decomposition temperature of InN during growth.[7]

In contrast to its thin film counterpart, freestanding one-dimensional (1D) nanostructures are easier to grow in single-crystal forms without defects, and hence lasing in the crystals could be more expected. Currently, various InN nanostructures, such as nanocrystals,[8] nanocolumns,[9] nanorods,[10] nanowires,[11] nanotubes,[12] nanotips,[13] and nanobelts,[14] have been extensively reported. Noticeably among these, InN nanobelts grown by a guided-stream thermal chemical vapor deposition (GSCVD) technique have shown a sharp infrared photoluminescence (PL) emission with a full width at half maximum (FWHM) of ~14 meV at 20 K, along with a linewidth narrowing at high excitation power, which was attributed to amplified spontaneous emission (ASE).[14] The onset of the ASE in the GSCVD-derived InN nanobelts sheds some light on the possibility of lasing if a proper cavity is present. Similar lasing behaviors in a variety of 1D nanostructures including ZnO, GaN, CdS, and ZnS have been observed.[15] In light of the above, in this letter, we report the observation of infrared lasing in high quality single-crystalline InN nanobelts fabricated by metal organic chemical vapor deposition (MOCVD). The realization of infrared lasing in InN nanobelts enables miniaturized IR laser light sources and opens up opportunities in the area of optical communication, gas sensors, and life sciences.

InN nanobelts were grown on Si (100) substrates in a homemade MOCVD reactor using trimethylindium and ammonia (NH_3) as the source materials of indium and nitrogen, respectively, while purified nitrogen was used as the carrier gas. For better optical confinement, the same growth was also conducted later on Si (100) substrates but coated with a thin amorphous silicon nitride (a-SiN_x) layer (~200 nm) using low-pressure chemical vapor deposition. Prior to growth, both two kinds of substrates were deposited a thin layer of gold film (2 nm), as the catalytic layer, with a direct current sputter (Emitech, K550X). The synthesis of InN nanobelts was all performed at the temperature of 540 °C and the pressure of 1 Torr for 4 h.

After growth, blackish products with a beltlike morphology were found to cover the entire substrates (2×2 cm^2), regardless of the presence of the a-SiN_x layer on the silicon substrates. The beltlike morphology of the products was confirmed using field emission scanning electron microscopy (FESEM) on a JEOL 6700 system. X-ray diffraction (XRD) on a Toshiba model A-40-Cu and transmission electron microscopy (TEM) on a high resolution JEOL model JEM-4000EX were employed to investigate the microstructure of the nanobelts. PL studies were performed at 20 K in a closed-cycle refrigerator system by using the 488 nm line of an Ar^+ laser as the excitation source and an InGaAs detector was used to record the spectra in the IR range.

Figure 1(a) shows typical FESEM images of the InN nanobelts grown on Si(100), which basically have the same morphology as that grown on a-SiN_x coated silicon. Clearly, high density nanobelts with lengths in the range of 15–62 μm can be observed. As shown in the high-

a)Authors to whom the correspondence should be addressed.
b)Electronic mail: chenkh@pub.iams.sinica.edu.tw
c)Electronic mail: chenlc@ntu.edu.tw

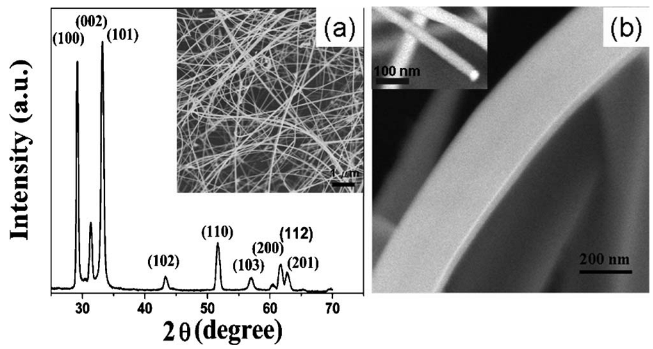

FIG. 1. (a) Typical XRD spectrum of MOCVD-grown InN nanobelts. The inset shows low-magnification SEM image of InN nanobelts. (b) High-magnification SEM image of a single InN nanobelt with well-defined facets and the observation of metallic nanoparticles attached at the growth front ends of InN nanobelts (inset.)

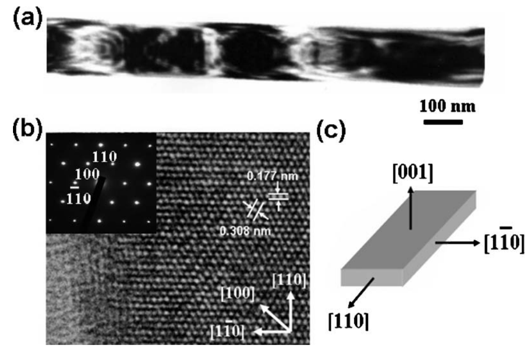

FIG. 2. (a) Low-magnification TEM image of a single InN nanobelt. (b) HRTEM image of InN nanobelt and corresponding selected area diffraction pattern (inset) of taken from the [001] zone axis. (c) Schematic diagram of the nanobelt crystallographic directions.

magnification FESEM image of Fig. 1(b), the nanobelts have well-faceted morphologies and atomically smooth surfaces, and have widths ranging from 40 to 250 nm and thicknesses from 10 to 35 nm. The observation of the catalytic nanoparticles attached at the growth front ends, as shown in Fig. 1(c), strongly supports that the growth of nanobelts is dominated by the vapor-liquid-solid (VLS) growth mechanism. XRD spectrum of the nanobelts was shown in Fig. 1(d). The diffraction peaks can be well indexed based on the hexagonal structure of InN, with lattice constants of $a=0.353$ nm and $c=0.570$ nm, which are in agreement with the standard literature values of $a=0.354$ nm and $c=0.571$ nm.[16]

Microstructure of the MOCVD-derived InN nanobelts was further characterized by TEM. Figure 2(a) shows a typical TEM bright-field image of the InN nanobelts. The dark fringes on the nanobelts result from bending contours, which are normally observed in bent thin crystals by TEM. The corresponding high resolution TEM (HRTEM) image of the nanobelt is shown in Fig. 2(b), which reveals the hexagonal structure of InN nanobelts with interplanar spacings of 0.177 and 0.308 nm along the [110] and [100] directions, respectively. Shown in the inset of Fig. 2(b) is the typical selected area electron diffraction pattern recorded along the [001] zone axis of the hexagonal InN. The clear spotty pattern indicates the single-crystal nature of the nanobelts. The above TEM studies concluded that the InN nanobelts were grown along the [110] direction and were enclosed by $\pm(001)$ and $\pm(1\bar{1}0)$ facets, as depicted in Fig. 2(c). Furthermore, it should be emphasized that InN nanobelts grown on bare Si substrates and a-SiN_x coated Si substrates both exhibit identical crystallographic properties, including growth direction and side facets.

To explore the possibility of stimulated emission from InN nanobelts, power-dependent photoluminescences of InN nanobelts grown on a Si(100) substrate and an a-SiN_x coated Si(100) substrate were both carried out. Figure 3 shows the 20 K power-dependent PL spectra of InN nanobelts grown on a Si substrate. At low excitation intensity, i.e., 10 kW/cm^2, a single broad spontaneous emission band with a FWHM of ~33 nm at 1600 nm was observed, which corresponded to the near band edge emission of InN. Apparently, a progressive narrowing of the peak width from ~33 to 17 nm associated with an enhancement of PL intensity can be clearly seen as the excitation power increases from 10 to 77 kW/cm^2. The peak narrowing could be attributed to the effect of ASE similar to the case observed in the GSCVD grown nanobelts.[14] Note that further increasing the pump power would only lead to structural damage of the nanobelts and no lasing behavior was observed. We have ascribed the reason to the poor light confinement of the nanobelts at the InN/Si(100) interface, since the refractive index of silicon ($n_{si}=3.47$) (Ref. 17) was much larger than that of InN ($n_{InN}=2.9$) (Ref. 18). Please refer to the report of Maslov and Ning[19] for a detailed discussion about the reflectivities, gain threshold, and lasing modes of nanowires.

For better light confinement, the a-SiN_x coated Si(100) substrate, where $n_{a\text{-}SiN_x}=1.9$,[20] was employed. Eventually, the lasing behavior was observed, as summarized in Fig. 4. At low excitation intensity (<50 kW/cm^2), as shown in Fig. 4(a), the spectrum consisted of a single broad spontaneous emission band with a FWHM of ~30 nm at 1594 nm. As the pumping intensity increases up to 73 kW/cm^2, several sharp peaks representing multiple laser modes emerged in the spectra between 1559 and 1644 nm. The typical linewidth of the observed sharp emission peaks at the highest pumping intensity of 75 kW/cm^2 is ~2.3 nm, which is nearly 14 times narrower than that (~33 nm) of the spontaneous emission below the threshold. The pump-power-dependent PL intensity was summarized in the inset of Fig. 4(a), which showed clearly that above a threshold excitation intensity (I_p) of ~70 kW/cm^2, a strong superlinear dependence of the emission intensity (I_{st}) with $I_{st}=I_p^{4.9}$ was present, while the depen-

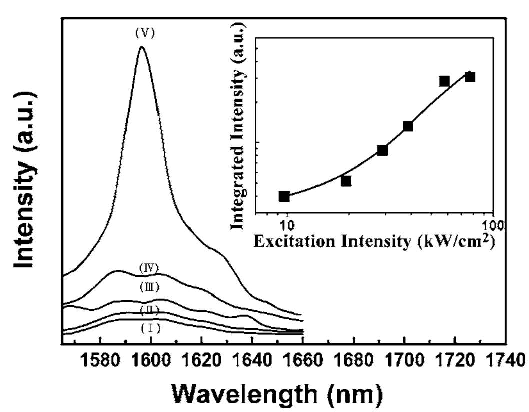

FIG. 3. Excitation power dependence of the emission spectra of InN nanobelts grown on Si substrates taken at 20 K. Excitation power was increased from 10, 19, 29, 39, and 77 kW/cm^2 for spectra (I), II, III, IV, and (V), respectively. The inset shows the integrated intensity as a function of excitation intensity.

dence of the spontaneous peak intensity was sublinear with $I_{st}=I_p^{0.83}$. The simultaneous superlinear dependence of the emission intensity and the linewidth narrowing at high pumping power [shown in Fig. 4(b)] suggests a transition from spontaneous emission to stimulated emission in the MOCVD-grown InN nanobelts.

Note here that for lasing in the InN nanobelts, a nanobelt cavity with effective reflectance on both ends is required. Though InN nanobelts were not vertically aligned with respect to the substrate, they were grown from the substrate, which enables good contact between the bottom end and the substrate. The observation of the lasing behavior from the InN nanobelts grown on the a-SiN_x coated silicon confirmed the fact that the waveguide structure based on the refractive index difference at the interface of air ($n_{air}=1$)/InN ($n_{InN}\sim 2.9$)/SiN_x ($n_{SiN_x}\sim 1.9$) facilitates better confinement and amplification of the light within the waveguide structure of air/InN/SiN_x for lasing action. This effect may be similar to the UV lasing action of ZnO nanoneedles grown on SiO_2 coated Si substrates, as reported by Lau *et al.*[21]

Assuming that the measured lasing modes were resulted from a Fabry-Pérot cavity, the cavity length (L) can be determined by $L=\lambda^2/2n\Delta\lambda$, where n is the refractive index and $\Delta\lambda$ is the mode spacing. Taking $n=2.9$ for InN and $\Delta\lambda=7$ nm, a cavity length of ~ 60 μm is required to sustain the observed lasing modes. This calculated cavity length falls well in the range of the length of nanowires measured by SEM. Figure 4(c) depicts another Fabry-Pérot cavity mode taken at a different site of the same sample, wherein an average mode spacing of 11 nm was observed, corresponding to a cavity length of 41 μm. According to a first approximation,[22] the gain threshold is proportional to $1/L$, thus leading to a lower lasing threshold for longer cavity length. In the present case, more than one cavity length was observed, suggesting that lasing takes place from InN nanobelts of different lengths. This fact also reflects the nonuniformity of nanobelt length. Furthermore, as shown in Fig. 4(a), a clear redshift of the gain profile was observed from 39 to 75 kW/cm^{-2}. The redshift of the gain profile could be induced by the band gap renormalization due to Coulomb interactions among amplified free carriers at the band edge. Similar redshift phenomena have been reported in 1D GaN (Ref. 23) or ZnO (Ref. 24) nanostructures. Another possibility of the redshift could be ascribed to the local heating of the nanowires, as high power densities of continue wave excitation were used in our study.

In summary, the infrared lasing from single-crystalline InN nanobelts was demonstrated in this study. TEM studies revealed that the rectangular cross-section InN nanobelts grew along the [110] direction and were enclosed only by $\pm(001)$ and $\pm(1\bar{1}0)$ planes. Infrared lasing action was observed at 20 K in InN nanobelts grown on SiN coated Si substrate by continuous wave laser pumping.

This research was financially supported by the Ministry of Education, Asian Office of Aerospace Research and Development under AFOSR, National Science Council of Taiwan, and Academia Sinica. The authors would like to thank S. H. Chang for fruitful discussions on random lasing. Technical support from the Academia Sinica Research Project on Nano Science and Technology is gratefully acknowledged.

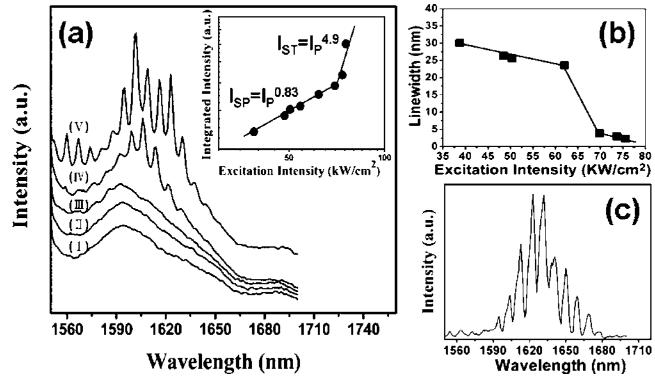

FIG. 4. (a) Power-dependent PL spectra of InN nanobelts grown on SiN coated Si substrates recorded at 20 K with excitation intensities of 39, 50, 62, 73, and 75 kW/cm^2 for PL spectra (I), II, III, IV, and (V), respectively. The inset shows the integrated intensity under different excitation intensities. (b) Linewidth of the emission peak as a function of excitation intensity. (c) Lasing spectrum obtained at different sites of the same sample as (a) at the excitation intensity of 77.5 kW/cm^2.

[1] B. E. Foutz, S. K. O'Leary, M. S. Shur, and L. F. Eastman, J. Appl. Phys. **85**, 7727 (1999).
[2] S. Chichibu, T. Azuhata, T. Sota, and S. Nakamura, Appl. Phys. Lett. **69**, 4188 (1996).
[3] K. P. O'Donell, R. W. Martin, and P. G. Middleton, Phys. Rev. Lett. **82**, 237 (1999).
[4] J. Wu, W. Walukiewicz, K. M. Yu, W. Shan, J. W. Ager, E. E. Haller, H. Lu, W. J. Schaff, W. K. Metzger, and S. Kurtz, J. Appl. Phys. **94**, 6477 (2003).
[5] J. Wu, W. Walukiewicz, K. M. Yu, J. W. Ager III, E. E. Haller, H. Lu, W. J. Schaff, Y. Saito, and Y. Nanishi, Appl. Phys. Lett. **80**, 3967 (2002).
[6] T. V. Shubina, S. V. Ivanov, V. N. Jmerik, D. D. Solnyshkov, V. A. Vekshin, P. S. Kop'ev, A. Vasson, J. Leymarie, A. Kavokin, H. Amano, K. Shimono, A. Kasic, and B. Monemar, Phys. Rev. Lett. **92**, 117407 (2004).
[7] A. G. Bhuiyan, A. Hashimoto, and A. Yamamoto, J. Appl. Phys. **94**, 2779 (2003).
[8] Y. J. Bai, Z. G. Liu, X. G. Xu, D. L. Cui, X. P. Hao, X. Feng, and Q. L. Wang, J. Cryst. Growth **241**, 189 (2002).
[9] C. L. Hsiao, L. W. Tu, M. Chen, Z. W. Jiang, N. W. Fan, Y. J. Tu, and K. R. Wang, Jpn. J. Appl. Phys., Part 2 **44**, L1076 (2005).
[10] C. H. Shen, H. Y. Chen, H. W. Lin, S. Gwo, A. A. Klochikhin, and V. Yu. Davydov, Appl. Phys. Lett. **88**, 253104 (2002).
[11] C. H. Liang, L. C. Chen, J. S. Hwang, K. H. Chen, Y. T. Hung, and Y. F. Chen, Appl. Phys. Lett. **81**, 22 (2002).
[12] L. W. Yin, Y. Bando, D. Golberg, and M. S. Li, Adv. Mater. (Weinheim, Ger.) **16**, 1833 (2004).
[13] S. C. Shi, C. F. Chen, G. M. Hsu, J. S. Hwang, S. Chattopadhyay, Z. H. Lan, and L. C. Chen, Appl. Phys. Lett. **87**, 203103 (2005).
[14] M. S. Hu, W. M. Wang, T. T. Chen, L. S. Hong, C. W. Chen, C. C. Chen, Y. F. Chen, K. H. Chen, and L. C. Chen, Adv. Funct. Mater. **16**, 537 (2006).
[15] P. J. Pauzauskie and P. Yang, Mater. Today **9**, 36 (2006).
[16] JCPDS Card No. 02-1450 (unpublished).
[17] M. Herzberger and C. D. Salzberg, J. Opt. Soc. Am. **52**, 420 (1962).
[18] H. Ahn, C. H. Shen, C. L. Wu, and S. Gwo, Appl. Phys. Lett. **86**, 201905 (2005).
[19] A. V. Maslov and C. Z. Ning, Appl. Phys. Lett. **83**, 1237 (2003).
[20] H. Akazawa, Appl. Phys. Lett. **80**, 3102 (2002).
[21] S. P. Lau, H. Y. Yang, S. F. Yu, H. D. Li, M. Tanemura, T. Okita, H. Hatano, and H. H. Hng, Appl. Phys. Lett. **87**, 013104 (2005).
[22] X. H. Han, G. Z. Wang, Q. T. Wang, L. Cao, R. B. Liu, B. S. Zou, and J. G. Hou, Appl. Phys. Lett. **86**, 223106 (2005).
[23] J. C. Johnson, H. J. Choi, K. P. Kuntsen, R. D. Schaller, P. Yang, and R. J. Saykally, Nat. Mater. **1**, 106 (2002).
[24] J. H. Choy, E. S. Jang, J. H. Won, J. H. Chung, D. J. Jang, and Y. W. Kim, Adv. Mater. (Weinheim, Ger.) **15**, 1911 (2003).